
Article:
Shukhobodskaia, D., Shukhobodskiy, A.A., Nelson, C.J. et al. (2 more authors) (2021) Significance of cooling effect on comprehension of kink oscillations of coronal loops. Frontiers in Astronomy and Space Sciences, 7. 579585. ISSN 2296-987X

https://doi.org/10.3389/fspas.2020.579585

---

frontiers in Astronomy and Space Sciences

ORIGINAL RESEARCH
published: 14 January 2021
doi: 10.3389/fspas.2020.579585

Significance of Cooling Effect on Comprehension of Kink Oscillations of Coronal Loops

Daria Shukhobodskaia[1], *Alexander A. Shukhobodskiy*[2], *Chris J. Nelson*[3], *Michael S. Ruderman*[1,4] *and Robert Erdélyi*[1,5]*

[1]Solar Physics and Space Plasma Research Centre (SP2RC), School of Mathematics and Statistics, University of Sheffield, Sheffield, United Kingdom, [2]School of Build Environment, Engineering and Computing, Leeds Beckett University, Leeds, United Kingdom, [3]Astrophysics Research Centre (ARC), School of Mathematics and Physics, Queen's University, Belfast, United Kingdom, [4]Laboratory of Interplanetary Medium, Space Research Institute (IKI) Russian Academy of Sciences, Moscow, Russia, [5]Department of Astronomy, Eötvös Loránd University, Budapest, Hungary

OPEN ACCESS

Edited by:
Valery M. Nakariakov,
University of Warwick,
United Kingdom

Reviewed by:
Pankaj Kumar,
Goddard Space Flight Center,
National Aeronautics and Space Administration, United States
David James Pascoe,
KU Leuven, Belgium

***Correspondence:**
Robert Erdélyi
robertus@sheffield.ac.uk

Specialty section:
This article was submitted to Stellar and Solar Physics, a section of the journal Frontiers in Astronomy and Space Sciences

Received: 02 July 2020
Accepted: 24 November 2020
Published: 14 January 2021

Citation:
Shukhobodskaia D, Shukhobodskiy AA, Nelson CJ, Ruderman MS and Erdélyi R (2021) Significance of Cooling Effect on Comprehension of Kink Oscillations of Coronal Loops. Front. Astron. Space Sci. 7:579585. doi: 10.3389/fspas.2020.579585

Kink oscillations of coronal loops have been widely studied, both observationally and theoretically, over the past few decades. It has been shown that the majority of observed driven coronal loop oscillations appear to damp with either exponential or Gaussian profiles and a range of mechanisms have been proposed to account for this. However, some driven oscillations seem to evolve in manners which cannot be modeled with purely Gaussian or exponential profiles, with amplification of oscillations even being observed on occasions. Recent research has shown that incorporating the combined effects of coronal loop expansion, resonant absorption, and cooling can cause significant deviations from Gaussian and exponential profiles in damping profiles, potentially explaining increases in oscillation amplitude through time in some cases. In this article, we analyze 10 driven kink oscillations in coronal loops to further investigate the ability of expansion and cooling to explain complex damping profiles. Our results do not rely on fitting a periodicity to the oscillations meaning complexities in both temporal (period changes) and spatial (amplitude changes) can be accounted for in an elegant and simple way. Furthermore, this approach could also allow us to infer some important diagnostic information (such as, for example, the density ratio at the loop foot-points) from the oscillation profile alone, without detailed measurements of the loop and without complex numerical methods. Our results imply the existence of correlations between the density ratio at the loop foot-points and the amplitudes and periods of the oscillations. Finally, we compare our results to previous models, namely purely Gaussian and purely exponential damping profiles, through the calculation of χ^2 values, finding the inclusion of cooling can produce better fits in some cases. The current study indicates that thermal evolution should be included in kink-mode oscillation models in the future to help us to better understand oscillations that are not purely Gaussian or exponential.

Keywords: solar corona, coronal loop oscillations, magnetohydrodynamics, kink oscillations, waves

1 INTRODUCTION

Standing, driven kink-mode oscillations within coronal loops have been extensively studied by the community ever since they were detected in the solar atmosphere at the end of the 20th Century (Aschwanden et al., 1999; Nakariakov et al., 1999) and for reviews see e.g. Andries et al. (2009); Ruderman and Erdélyi (2009). It is now known that, typically, flare-driven kink-mode oscillations are observed to damp within only a few periods, faster than would routinely be expected given the large amplitudes present (see, for example, Aschwanden and Terradas 2008), implying the presence of complex physics during these relatively routine events. The damping profiles of the majority of driven kink-mode oscillations can be well fitted by either Gaussian or exponential profiles (as shown in the statistical study of Goddard et al., 2016) and numerous physical mechanisms have been proposed to account for such decay. Resonant absorption is one such mechanism and has been widely analyzed in numerous analytical works with the aim of better understanding damping within kink-mode oscillations. (e.g., Goossens et al., 2002; Ruderman and Roberts 2002; Dymova and Ruderman 2006; Shukhobodskiy and Ruderman 2018). Interestingly, resonant absorption was proposed well before the first direct detection of kink-modes in coronal loops in the solar atmosphere (Hollweg and Yang 1988; Goossens et al., 1992; Erdelyi and Goossens 1994, Erdelyi and Goossens 1995). The potential transition from Gaussian to exponential damping during the course of a single coronal loop oscillation for propagating kink waves was derived by Hood et al. (2013) in the absence of cooling and for standing kink waves by Ruderman and Terradas (2013). For a review on resonant absorption without complex profiles in a solar context see Goossens et al. (2011).

The improvement in both the spatial and temporal resolutions of coronal imaging which resulted from the launch of the Solar Dynamics Observatory's Atmospheric Imaging Assembly (SDO/AIA; Lemen et al., 2012) in 2010 has facilitated major advances in understanding of coronal loop oscillations over the past decade. For example, it is now known that multiple harmonics can be present in kink-mode oscillations (Pascoe et al., 2016a), that decay-less observations are present in some coronal loops (Anfinogentov et al., 2013), and that coronal loops can be multi-thermal in nature (Krishna Prasad et al., 2017). One of the main benefits of the continuous, full-disk observations provided by the SDO/AIA instrument is that large statistical studies of coronal loop oscillations can now be conducted (see, e.g., Zimovets and Nakariakov 2015; Goddard et al., 2016). Goddard et al. (2016), for example, studied 120 kink-mode oscillations finding parameters such as amplitudes, damping times, and periods. Ground-based facilities also enable such statistical investigations in chromospheric wave-guides, as were conducted by Kuridze et al. (2012), Morton et al. (2012) who studied the properties of transverse oscillations in mottles. Furthermore, for the example of undamped kink oscillations presented by Aschwanden and Schrijver (2011), Kumar et al. (2013) showed that such phenomena could be triggered by the combination of fast and slow MHD waves present within the system. Moreover, Wang et al. (2012) suggested that amplification could occur due to additional energy input, potentially associated with flaring during the lifetime of the initial oscillation (Pascoe et al., 2020).

Such studies are highly valuable and provide important constraints which can help with the verification of numerical and analytical theories. Interestingly, although the evolution of the majority of coronal loop oscillations analyzed by Goddard et al. (2016) could be modeled using Gaussian, exponential, or Gaussian followed by exponential fits, 21 decaying kink-mode oscillations were identified which had combinations of both exponential and non-exponential damping profiles co-temporally. The presence of these complex or non-standard damping profiles, which cannot be approximated by a few Gaussian profiles and exponential profiles attached to each other in a definite order, sometimes including amplification of the oscillations through time, implies further work is required to fully understand what effects are important in defining the evolution of kink-modes in some coronal loops.

The first analytical models of kink oscillations of coronal loops were simple and considered homogeneous magnetic flux tubes (e.g. Ryutov and Ryutova 1976; Edwin and Roberts 1983). More recently, the idea of analytically studying cooling effect on MHD waves (see e.g. Morton et al., 2010) and in particular on the seismological properties for kink oscillations of coronal loops (see Morton and Erdélyi 2009; Morton and Erdélyi 2010) was proposed. Morton and Erdélyi (2010); Ruderman (2011a) concluded that in the absence of damping due to resonant absorption cooling can cause amplification of coronal loops. Furthermore Ruderman (2011b) concluded that combining cooling and resonant damping can result in the amplitude not varying in time (i.e., the oscillation being decay-less). Ruderman et al. (2017) studied the combination of cooling and expansion for non damped kink oscillation, it was shown that expansion of coronal loops acts in favor of amplification. Shukhobodskiy et al. (2018) considered the similar problem in the presence of damping due to resonant absorption and found that the combination of cooling and expansion can lead to an increase in the oscillation amplitude even in presence of resonant damping. The theory was later tested observationally by Nelson et al. (2019) on one kink-mode oscillation. It was found that increases in the amplitude of the oscillation through time could be explained if cooling was considered, without the need of external forces (e.g., additional flaring) affecting the oscillating system in order to sustain oscillation.

Cooling has been observed in many coronal loops during their lifetimes and has numerous observational signatures, both direct and indirect. The most direct signature is the visible transition of the loops from channels sampling hotter plasma to channels sampling cooler plasma through time (as was shown by, for example, Winebarger and Warren 2005; López Fuentes et al., 2007; Aschwanden and Terradas 2008). More indirect mechanisms include coronal rain (e.g., Antolin et al., 2015) and associated process such as downflows in transition region spectra at the foot-points of coronal loops (Kleint et al., 2014; Ishikawa et al., 2020). Both coronal rain and transition region downflows have been shown to be stable (Antolin et al., 2015;

Straus et al., 2015) and variable (Antolin et al., 2015; Nelson et al., 2020a) over short time-scales meaning the thermal evolution of coronal loops may be an on-going and variable process throughout their lifetimes. It is known that transition region downflows occur above almost all sunspots (Samanta et al., 2018; Nelson et al., 2020b) implying that a high number of coronal loops do not maintain constant temperatures through time. The effects of thermal evolution (both heating and cooling) within loops should, therefore, be considered when analyzing the oscillations of coronal loops (see e.g., Morton et al., 2010; Erdélyi et al., 2011; Al-Ghafri and Erdélyi 2013; Al-Ghafri et al., 2014 to name a few studies).

In this article, we analyze 10 examples of kink mode oscillations in coronal loops which damp with non-Gaussian and non-exponential profiles, as identified in the statistical study of Goddard et al. (2016). Our aim is to understand whether a range of damping profiles can be explained using the theories develop in Shukhobodskiy et al. (2018) which accounts for cooling within the loops during the oscillations. We are not claiming that cooling occurs in the studied loops (this would need to be studied in more detail in a separate study) but are, instead, displaying the flexibility of the theory and offering a discussion of when it may be useful in understanding the solar atmosphere. Our work is laid out as follows: In **Section 2** we detail the coronal loops studied here and the data used to analyze them; In **Section 3** we present our results; Before in **Section 4** we draw our conclusions.

2 OBSERVATIONS—EVENT SELECTION AND MODEL FITTING

The aim of this article is to understand whether a range of damping profiles of kink mode oscillations can be explained by the effects of cooling and to compare this model to several other previously studied models. To tackle this aim, we selected 10 events randomly from the sample identified to damp with both exponential and non-exponential components in the statistical study of Goddard et al. (2016) for analysis. The combination of exponential and non-exponential components implies a level of complexity in the amplitude profiles through time which could be an observational signature of cooling. Each of these 10 examples of kink-mode oscillations were sampled by the SDO/AIA instrument at discrete times between November 3, 2010 and July 18, 2013, with the periods of these oscillations ranging from slightly over 2 min up to nearly 16 min. Here, we specifically study data from the 171 Å filter which samples the coronal plasma at temperatures of around 0.6 MK with a cadence of 12 s and a pixel scale of 0.6″. A 300″×300″ field-of-view (FOV) around each oscillation was downloaded for a 1-h time-series beginning 15 min before the oscillation was deemed to have begun in Goddard et al. (2016) using the *ssw_cutout_service.pro* routine. Frames from the SDO/AIA instrument can have reduced exposure times during flares resulting in frames being dropped during download. Therefore, we filled any gaps in the time-series with synthetic images generated by averaging the intensities in the previous and following frames at each pixel. Since no consecutive frames were dropped, this should have no effect on the identification and analysis of oscillations with periods of the order minutes. Time-distance diagrams were then constructed to mimic the slits studied in Goddard et al. (2016), with a width of five pixels. In **Table 1**, we detail the basic information of the 10 oscillations studied in this article. We should also note that Pascoe et al. (2017) have extensively studied density contrast for the event 40 02. Furthermore, comprehensive temporal analysis was performed by Goddard and Nisticò (2020) for the event 03 01.

In **Figure 1**, we plot the time-distance diagrams constructed for each of the events studied here (using the routine detailed in Krishna Prasad et al., 2012) over the course of 1 h. Each slit has a different length, however, they have all been scaled to the same y-axis to emphasize the oscillations. The blue dots over-laid on each panel indicate the edges of the loop, identified using the Canny edge-detection method in Wolfram Mathematica 12. The red dots in each panel indicate the mid-points between the detected edges that we infer to be the central axis of the oscillating loop here. The background trend was then accounted for by fitting a function, using spline fitting, through the averages between local extremum points, similar to the method described in Pascoe et al. (2016b). Once the background trend had been subtracted, the amplitudes of the oscillations were normalized and fitted with a sum of Gaussian profiles of the form:

$$f(\mathrm{amp}) = \sum_{i=1}^{n} A_i \exp\left[-\left(\mu_i + t\right)^2 \Big/ \left(2\sigma_i^2\right)\right] \Big/ \sqrt{2\pi}/\sigma_i^2, \qquad (1)$$

where A_i and μ_i, and σ_i are the amplitude, shift, and width of the profile fitted to each peak. The value of n corresponds to the number of extrema identified for each oscillation. To ensure that the summed functions maintain continuity, we used the Wolfram Mathematica 12 function *Non-linearModelFit*. The benefit of fitting Gaussians to each extrema profile independently is that no implicit periodicity needs to be assumed for the oscillations. All of these steps allow us now to estimate the damping profile of each oscillation that can be modeled using the theories described in Shukhobodskiy et al. (2018). The procedure described here is essentially similar to that used in Nelson et al. (2019), but with the exception of an updated background trend approximation.

3 RESULTS

3.1 Theoretical Model

In this article, we expand on the work of Nelson et al. (2019) by applying the model proposed by Shukhobodskiy et al. (2018) to analyze 10 complex kink-mode oscillations. Here, let us provide a brief summary of the theoretical model for completeness. We consider an expanding and cooling loop of semi-circular shape surrounded by an annulus layer which is fixed in the dense photosphere. We note that the effects of curvature are only applied to the density distribution meaning, essentially, we consider the loop to be a straight magnetic flux tube with radius $R(z)$ (including the annulus layer) and length L. The

TABLE 1 | Properties of the kink-mode oscillations studied here.

Event ID	Loop ID	Slit position [x1, y1, x2, y2] (arcsec)	Date	Time UT	Period (min)	Osc amp (mm)
03	01	−977, −383, −988, −368	2010-Nov-03	12:13:48	2.46 ± 0.03	4.7
03	02	−970, −416, −1001, −393	2010-Nov-03	12:14:35	3.62 ± 0.08	9.7
04	01	912, 405, 889, 433	2011-Feb-09	01:30:02	2.29 ± 0.03	4.4
26	01	1098, 13, 1126, 51	2012-Jan-16	00:08:28	11.95 ± 0.13	9.2
40	02	−1077, −121, −1065, −96	2012-Oct-20	18:09:33	5.61 ± 0.03	4.4
40	04	−1045, −114, −1020, −110	2012-Oct-20	18:10:08	5.53 ± 0.04	2.5
40	07	−1107, −153, −1094, −121	2012-Oct-20	18:11:11	5.72 ± 0.06	3.4
40	08	−1036, −217, −1066, −194	2012-Oct-20	18:08:39	4.33 ± 0.08	12.1
43	05	801, 608, 812, 631	2013-Jan-07	06:37:11	4.5 ± 0.02	2.2
48	01	−1076, 77, −1044, 111	2013-Jul-18	17:59:56	15.28 ± 0.16	22

The information given is in the same format as in Table A1 from Goddard et al. (2016) for consistency with the previous literature. Note the estimation of period and apparent oscillation amplitude (later in the text we do not use the word "apparent" in front of the amplitude) are from Goddard et al. (2016) and are not estimated directly in this article. These are included for comparison with ***Figure 2****.*

temperature of the loop is assumed to decay exponentially through time (similarly to, for example, Aschwanden and Terradas 2008; Morton and Erdélyi 2010; Ruderman et al., 2017; Ruderman et al., 2019) following:

$$T(t) = T_0 \exp(-t/t_{\text{cool}}), \tag{2}$$

where T_0 is the constant external temperature and t_{cool} is the cooling time. We assume that the cooling time is equal to the total lifetime of the oscillation in each case studied.

The variation of the loop cross-section, $R(z)$, is defined by the relation:

$$R(z) = R_f \lambda \sqrt{\frac{\cosh(L/2L_c) - 1}{\cosh(L/2L_c) - \lambda^2 + (\lambda^2 - 1)\cosh(z/L_c)}}, \tag{3}$$

where z is the height of the tube (set to be equal to 0 at the apex), R_f is the radius of the magnetic flux tube at the foot-point, $\lambda = R(0)/R_f$ is the expansion factor of the loop, and L_c is an arbitrary constant. This radius profile was also considered by Ruderman et al. (2008), Ruderman et al. (2017) and Nelson et al. (2019). The density is set to transition from the internal value to the external value in the annulus layer. We follow Goossens et al. (2002) and Shukhobodskiy and Ruderman (2018) and assume that density in the annulus region where resonant absorption can occur, ρ_t, can be modeled linearly as:

$$\rho_t = \frac{\rho_i + \rho_e}{2} + (\rho_i - \rho_e)\frac{R - r}{lR}, \tag{4}$$

where ρ_i is internal density, ρ_e is external density, r is the radial component, where $r = 0$ at the center of the magnetic flux tube, and l is a dimensionless parameter, such that $lR(z)/2$ is the radius of the transitional layer.

With the aid of **Eqs 2–4**, Shukhobodskiy et al. (2018) derived the relation for the dimensionless amplitude, $A(t)$, where $A(0) = 1$, of the kink mode under the thin tube and thin boundary approximation. In addition to λ, below are the most important parameters in the model:

$$\zeta = \frac{\rho_i(\pm L/2)}{\rho_e(\pm L/2)}, \quad \kappa = \frac{L}{\pi H_0} \text{ and } \alpha = \frac{\pi l C_f t_{\text{cool}}}{4L}, \tag{5}$$

where H_0 is the scale height in the exterior plasma and C_f is the kink speed at the foot-points of the loop. The parameter ζ corresponds to the ratio between the internal and external densities at the loop foot-points, κ corresponds to the ratio between the coronal loop length and the plasma scale height in the region outside the loop, and, finally, α represents the relative strength between damping due to resonant absorption and amplification due to cooling. In the case where $\alpha = 0$ there is no damping. Furthermore, the ratio of densities at any point of the loop is defined by Eqs 71–73 derived by Shukhobodskiy et al. (2018).

We note that to obtain results for comparison with observed amplitude profiles, the arbitrary constant, L_c should be carefully selected such that the expansion factor be in line with observed values ($1 < \lambda < 1.5$; Klimchuk 2000; Watko and Klimchuk 2000). Here, we set $L/L_c = 6$ (similarly to Ruderman et al., 2008; Shukhobodskiy et al., 2018 and Nelson et al., 2019) to achieve this aim. We also set $A_t = A(0)A_{Ob}(0)$, where A_{Ob} is the initial amplitude measured of the observed oscillation and A_t is the scaling factor for the dimensionless amplitude. This would enable us to compare analytical and theoretical results within comparable scale.

3.2 Results of the Model Fitting

In order to fit these observations with the model, we first need to obtain the damping profiles for each of the 10 events studied here. In **Figure 2**, we plot each of the oscillations identified in **Figure 1** with red dots. Each of these oscillations appears to be qualitatively different with different periods and amplitudes, with some having large amplitudes and some only appearing to have small amplitudes (only several pixels). This variety in the studied oscillations allows us to test the model in a more dynamic

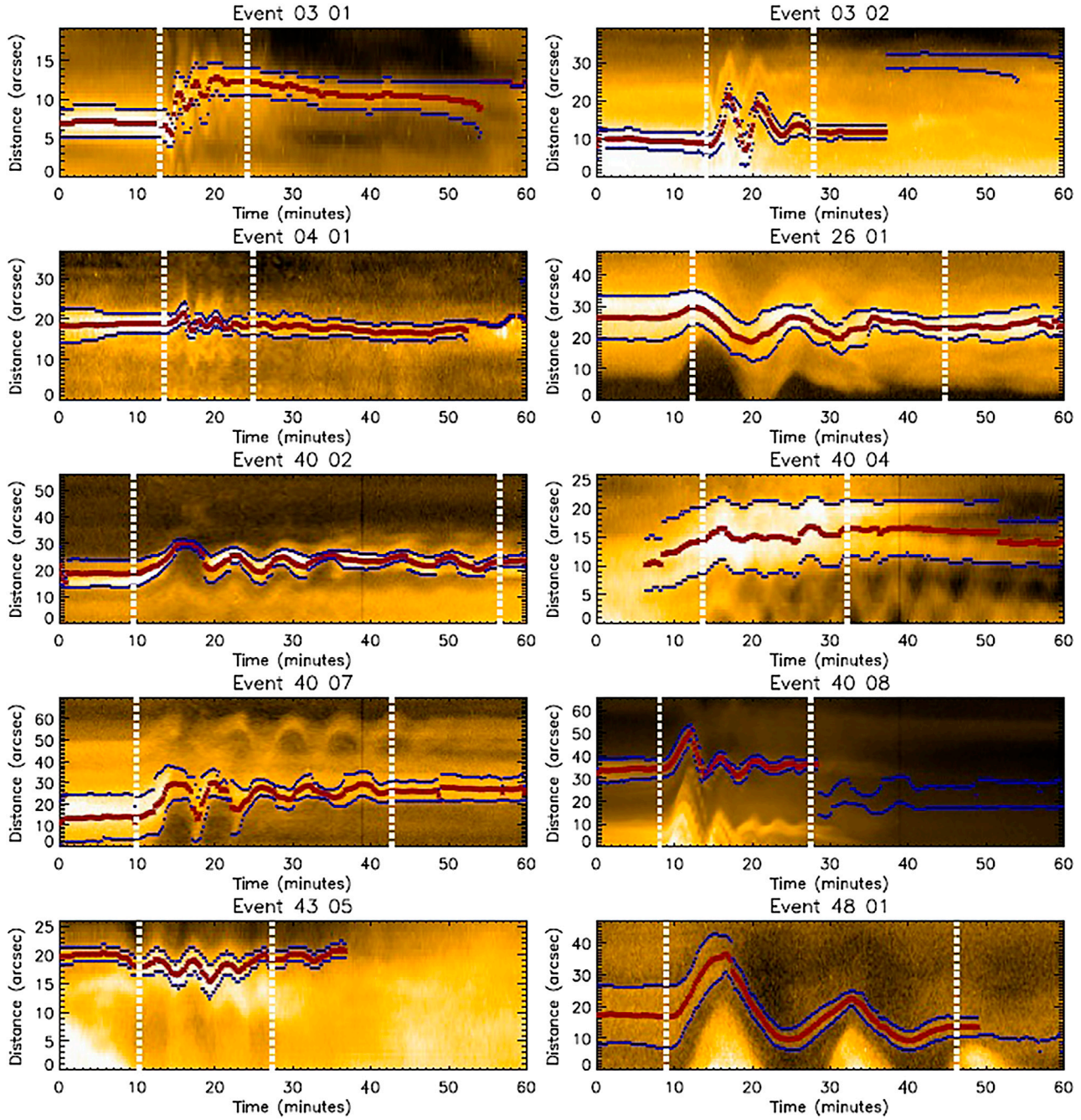

FIGURE 1 | Time-space diagrams for each of the selected events studied here. The *x*-axis of each panel corresponds to 1 h. The *y*-axes are all different in lengths but are scaled independently to improve the visibility of the oscillations. Exact timing and distance information is provided in **Table 1**. The results of the Canny edge-detection algorithm are over-laid as blue crosses. The central position between these points, assumed to be the center of the loop axis through time, is signified by the red crosses. The vertical white dashed lines denote the time-period plotted in **Figure 2**. We note that Event 40 04 could correspond to two individual loops overlying each other, however, we do not remove it as the complex amplitude profile allows us to show-case both the strengths and limitations of the method.

way than if all oscillations displayed similar behavior. With this in mind, we keep the fitting of Event 40 04 despite the apparent overlap between two independent loops in the slit and label this as a "low-confidence" [LC] event in the remainder of this article. The green and blue lines in **Figure 2** mark the spline fits (following the method of Pascoe et al., 2016b) and the results of applying **Eq. 1**, respectively, for each of the events. The dashed black vertical lines indicate the temporal regions of interest within which the oscillations were studied in the remainder of this article. The next step in our analysis was

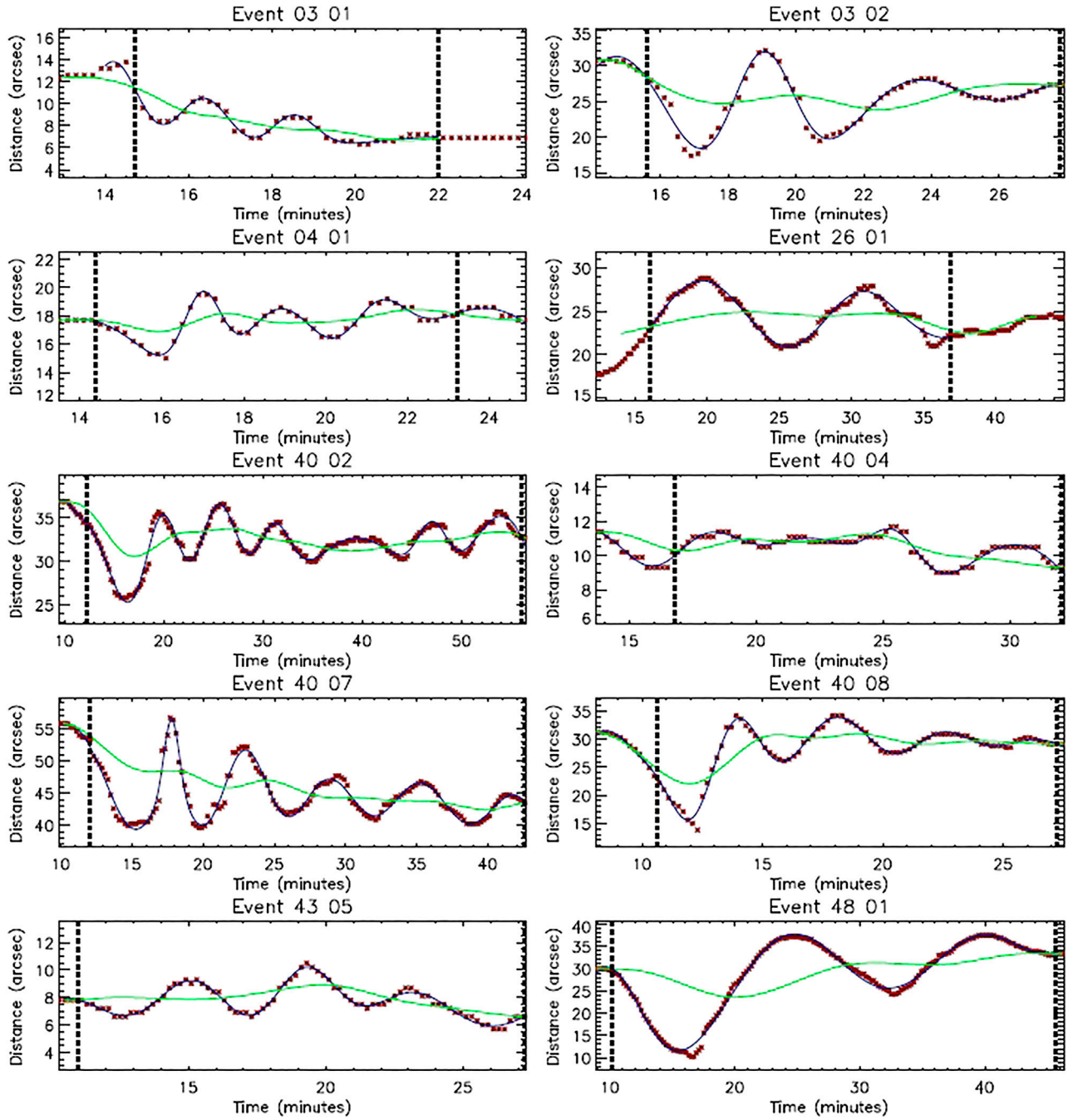

FIGURE 2 | Displacement profile of each coronal loop studied in this article. The red points correspond to the red points over-laid on **Figure 1** and track the measured amplitudes of the oscillation. The green lines display the background trend estimated using spline fitting. The blue lines are the results of fitting **Eq. 1** to each oscillation. Note the ability of this method to deal with variable periodicities, best seen in Events 40 02 and 40 07. The dashed black vertical lines on each panel outline the time-period plotted in Figure 3.

to remove the effects of the background trends and normalize the amplitudes such that the damping profiles could be calculated. The results of this procedure are plotted in **Figure 3**. It is immediately evident that the damping profiles of Events 03 01, 04 01, 40 02, 40 04 (LC), 40 07, 40 08 and 43 05 clearly deviate from both typical exponential and Gaussian damping. Some of these events display an increase in the amplitude through time whilst some others have stagnation periods where the amplitude remains constant for a while before further amplitude reduction takes place. Such damping profiles are difficult to explain using standard methods.

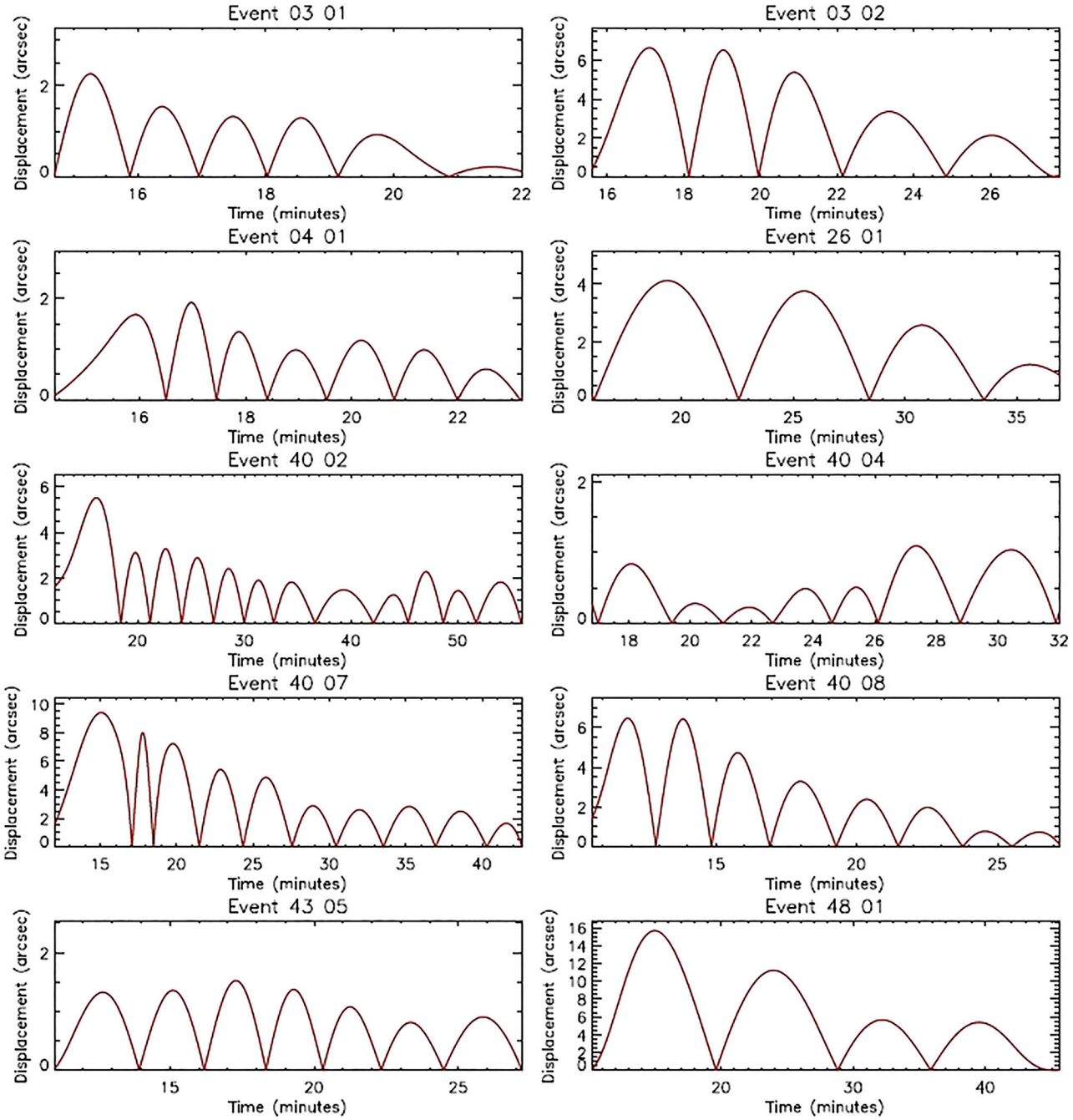

FIGURE 3 | The absolute value of the displacement of the Gaussian fitted position profiles (blue line from **Figure 2**) from the spline fitted background trend (green line from **Figure 2**) through time for each of the events studied here.

Next, we applied the model proposed by Shukhobodskiy et al. (2018) to the damping profiles, varying the four parameters discussed in the previous section to minimize the departure from the measured amplitude profile (as was previously done by Nelson et al., 2019). In **Figure 4** we plot the amplitudes of each peak of each oscillation as green dots, with spline fits over-laid as blue lines. The optimized results of the model fitting are over-laid as red lines. In order to compare with other single models, we also plot fits calculated using both exponential (dashed) and Gaussian (dot-dashed) profiles, as discussed in Pascoe et al. (2016b), which study the damping of a fundamental mode. The parameters used for the cooling model provide sufficiently good fits in a qualitative sense in the majority of cases, as can be seen in **Figure 4**, with only Event 40 04 (LC) being visually poorly fitted. Essentially, including the effects of cooling in the fitting of kink-mode damping profiles can produce good fits for a wide variety of

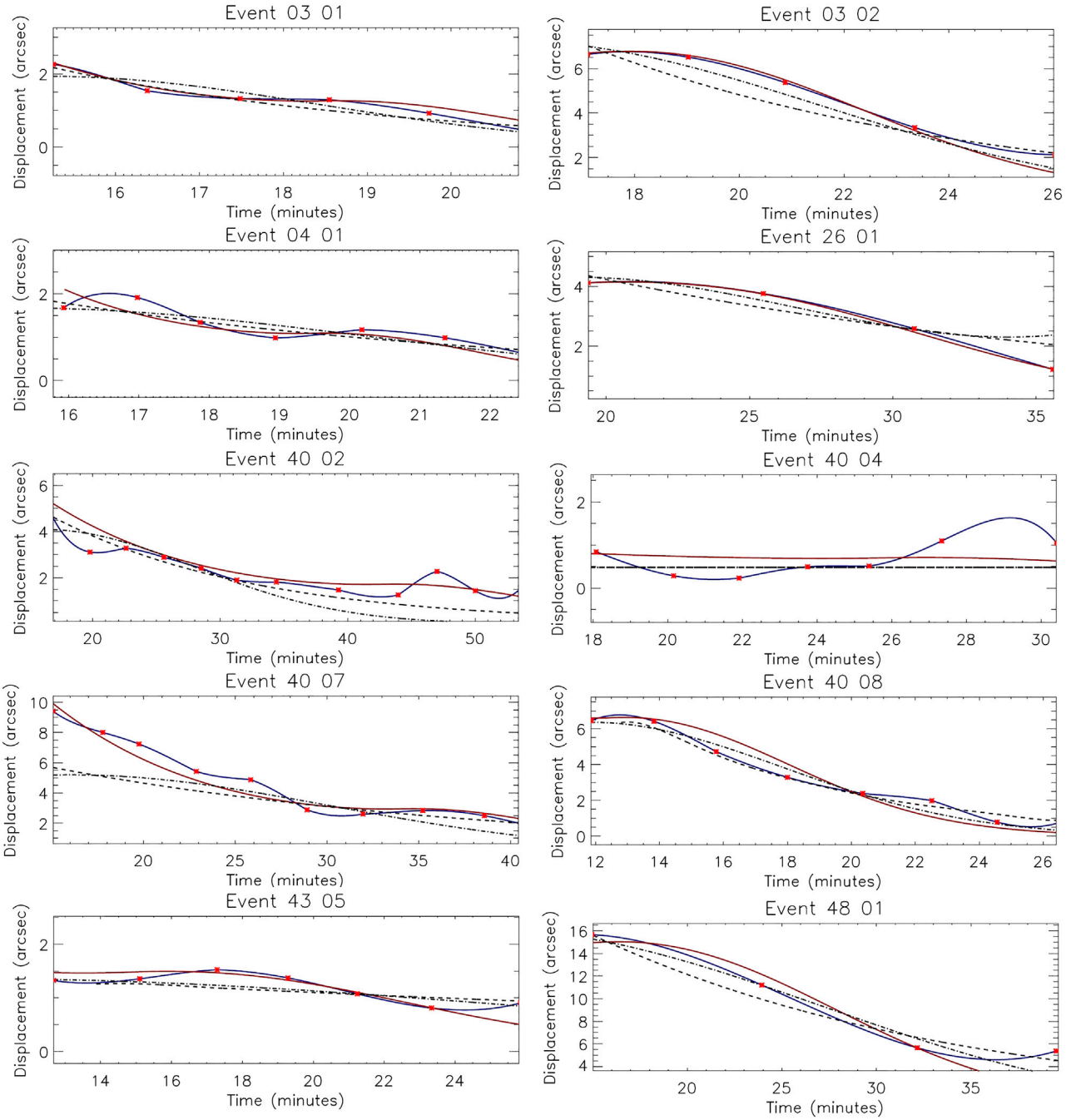

FIGURE 4 | The fitting of the model, introduced by Shukhobodskiy et al. (2018), to the coronal loop oscillations studied here. The blue lines plot spline fits through the maxima of each peak plotted in **Figure 3**. The red lines plot the approximation of the oscillations obtained through fitting the theoretical model. Reasonable fits are achieved for all events except Event 40 04 (LC). The dot-dashed lines represents Gaussian fit and the dashed lines correspond to exponential fits. Finally, the red crosses indicate the peaks from **Figure 3**.

profiles but even this method can struggle when low amplitude, highly variable damping profiles are considered. Deviations from standard Gaussian or exponential damping profiles are most prominent in Events 03 01, 03 02, 04 01, 26 01, 40 07 and 43 05 where several saddle points are evident in the fits. It is worth noting that this model is also capable of capturing features of both the Gaussian and exponential damping profiles by varying its parameters, with near-Gaussian damping profiles being returned for Events 40 08 and 48 01 and near-exponential damping being returned for Event 40 02. We note that Gaussian damping profiles can only be obtained for low values of ζ (< 1.2) whereas exponential damping profiles can only be obtained with values

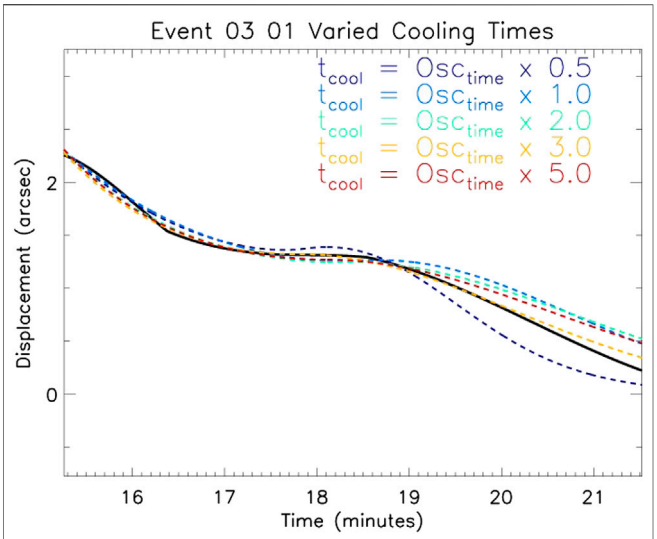

FIGURE 5 | Examination of the effect of cooling time on the fits of the analytical model to observations. The κ values for each of the cooling times (from quickest to slowest) are 1.3, 2.9, 5.6, 5.7, 10.9, respectively, and the corresponding ζ values are 3.7, 3, 1.7, 1.35, 1.2. We should note the condition of applicability of Shukhobodskiy et al. (2018) is $t_{cool} \gg P/6$, where t_{cool} is the cooling time and P is oscillation period.

of ζ higher than 4.5 when values of κ, λ, and α are not extreme. For values of α closer to 0, the effect of damping due to resonant absorption would be completely canceled out by the amplification due to cooling with overall amplification present. On the other hand, high values of α would result in profiles very similar to exponential decay, due to strong damping accountable for resonant absorption and weak cooling, though small increases in amplitude would be still present. The specific value of α that would make this change is dependent on the loop itself. Lowering the loop length by making κ smaller will compensate the increase in α. Furthermore, higher loop expansion favors amplification, therefore, to reduce the damping profile to an exponential profile one would need to consider values of $\zeta > 7$.

Highly complex amplitude profiles, for example Event 43 05, display both decreases and increases in the amplitude through time. Fortunately, this complexity can be explained by theory once cooling is considered. For lower values of ζ less than 1.2 the theoretical profile reduces to Gaussian decay. Whereas, for higher values of density ratios, the initial part would start with exponential decrease first and then after some time the local increase may appear after which the Gaussian decay profile appears. This behavior provides higher degrees of freedom in fitting the observations meaning more amplitude profiles are now theoretically permitted. This fact makes it ultimately both convenient and useful to consider the evolution of temperature during oscillations for accurate approximation of seismological parameters. Goddard and Nakariakov (2016) discussed the importance of the projection angle in order to obtain more accurate information about coronal loops, which could cause a cascade of associated errors and require the need to perform multiple angle analysis of the same phenomena. Despite this fact, the model used in this article is not dependent of the absolute values of the damping profile, rather it depends on the normalized shape of oscillation, making it resistant to the above errors in obtaining the dimensionless parameters. As such, that could lead to faster analysis of kink oscillations of coronal loops. However, such an error does limit the estimation of parameters with dimensions in the model used here.

We should note that ζ is responsive to the position where the analytical solution changes it shape (e.g., where amplitude increases are detected). Any increases in the assumed cooling time results in a stretching of the analytical solution and lowers the value of ζ, however, such effects becomes slower or negligible as ζ becomes closer to 1 as seen in **Figure 5**. Additionally, increases in the cooling time lead to increases of κ in order to fit the observed shape. Nevertheless, in all occasions the model is able to capture the observed profile for various lengths of cooling. Essentially, this introduces some degeneracy in our solutions which will need to be further studied through future research. Moreover, oscillations with low values of ζ are barely affected by the cooling time, where kink oscillations with high values of ζ could lead to overestimation of this parameter and require additional measurements to determine t_{cool} or κ. Once t_{cool} or κ is known or measured the model provides quick and accurate estimate for ζ. Furthermore, in the case where values of ζ are in the range 1–1.7 existing estimates of damping profiles are sufficiently good even without knowing t_{cool} and κ. We should note that the theoretical model studied here explains deviations from typical exponential or Gaussian damping profiles due to cooling, which causes plasma flows toward footpoints of the coronal loop. As a result, the upper parts of the coronal loops become lighter, however the impulse is preserved. The lighter the loop with comparison to

TABLE 2 | Comparative analysis for goodness of fit from the observed data for the theoretical model presented by Shukhobodskiy et al. (2018) and for Gaussian and exponential fits presented by Pascoe et al. (2016b).

Event	χ_t^2	χ_g^2	χ_e^2	$\tilde{\chi}_t^2$	$\tilde{\chi}_g^2$	$\tilde{\chi}_e^2$
03 01	0.5692	0.6857	0.4702	3.8990	5.6609	4.1022
03 02	0.5312	1.1218	1.3095	7.7526	26.8841	26.8841
04 01	0.4909	0.2764	0.2810	5.4039	7.3583	5.3894
26 01	0.0086	0.0446	0.1781	0.9976	38.5140	33.9762
40 02	1.5567	9.7141	7.0435	110.7415	646.3610	242.6087
40 04	3.6473	2.7641	2.7642	150.7310	99.0152	99.0189
40 07	1.0192	9.4239	7.9315	50.3733	314.3506	292.3057
40 08	2.2148	0.9184	0.6627	68.0517	25.3550	28.0358
43 05	0.3280	0.2262	0.3118	4.6998	8.6158	12.9752
48 01	3.9506	2.5507	1.1667	168.46012	61.3025	89.8005
Event 03 01					$\tilde{\chi}_t^2$	$\tilde{\chi}_t^2$
Cooling time is equal to oscillation time × 0.5					0.2277	4.8311
Cooling time is equal to oscillation time × 2.0					0.7294	3.0602
Cooling time is equal to oscillation time × 3.0					0.1180	0.2628
Cooling time is equal to oscillation time × 5.0					0.5357	1.8411

χ_t^2, χ_g^2, and χ_e^2, correspond to χ^2 goodness of fit calculations for the cooling, Gaussian, and exponential models, respectively, only by comparing extremum points (i.e. peaks of the amplitudes). $\tilde{\chi}_t^2$, $\tilde{\chi}_g^2$, and $\tilde{\chi}_e^2$, correspond to $\tilde{\chi}^2$ goodness of fit for the cooling, Gaussian, and exponential models comparing overall fit at all times during the damping. The top panel exhibit the analysis for all studied events with cooling time being equal to oscillation time and bottom panel corresponds to the event 03 01 for various cooling times.

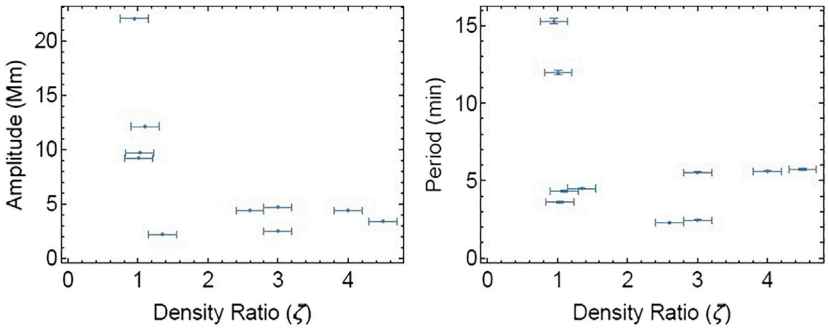

FIGURE 6 | Scatter plots displaying the apparent relationships between the amplitude and period of the coronal loop oscillations (as measured by Goddard et al., 2016) and the density ratio inferred here.

surroundings the less affect will be visible by cooling. That could be seen that for values of $\zeta < 1.2$ the damping profile is almost Gaussian. Furthermore the effect on heavier loops with $\zeta > 7$ is the similar, since the cooling time is not sufficient to affect the initial impulse of the oscillation. As a result, an exponential damping profile is preserved. Despite that, the introduction of cooling to the system might still provide better approximation for oscillations, however, at this time it is difficult to test this observationally. Furthermore, the most interesting analysis occurs for values of $1.2 \leq \zeta \leq 7$, where cooling plays a significant role in determining oscillation profiles. It is in this density range that future analyses could be focused.

The inferred, best fit, parameters (defined in the previous section) for each of the oscillations are presented in **Table 2**. To obtain accurate approximations for ζ, care should be taken in accurately positioning the dashed black lines in **Figure 2** due to its high sensitivity to temporal variations. In **Figure 6**, we plot the relationship between the density ratio at the loop foot-points, ζ, and the oscillation amplitudes (left panel) and periods (right panel) as measured by Goddard et al. (2016). It is immediately evident that the higher amplitude and longer period oscillations appear to have lower density ratios between the loop and the external environment at the foot-points. Although we are hesitant to draw strong conclusions about this due to the small statistical size and lack of direct density diagnostics, this result does suggest further research should be done to investigate such links in the future. Some important steps forward could come through analyzing the ratios between the O IV lines sampled by the Interface Region Imaging Spectrograph (IRIS; De Pontieu et al., 2014) at the foot-points of oscillating loops. Some limitations of this model are evident in **Figure 4** where deviations between the fitted theoretical model and the measured observed values are evident. It is unclear at this stage whether these limitations are caused by differences in the observed and modeled structures or due to measurement errors. It should be noted that the recent work of Goddard et al. (2017) shows that some of the loops might not have thin boundaries, with Pascoe et al. (2019) discussing the possible limitations of the thin boundary approximation used within theoretical approach. This could possibly lead to underestimation of ζ, with the current model supporting $l \leq 0.5$. However, the effect of the transitional layer changes have not yet being studied in this configuration for cooling loops to provide accurate estimates of possible errors for kink oscillations of cooling coronal loops with $l \geq 0.5$. Future observational and analytical work will be needed to better understand this. We also note that since the analytical model is very sensitive in a non-linear way to the position of local oscillation amplification, without significant improvement in image resolution, it would be impossible to obtain the estimate of an error of given ζ and consequently all other parameters. Thus an upper bound of general error estimates for fixed values of ζ are applied here. However, once the spatial resolution of obtained data increases and the shape observed oscillation is more certain, quantification of these errors will be paramount for correct estimates.

TABLE 3 | Best-fit parameters fitted by the theoretical model for each of the loop oscillations studied here.

Event	03 01	03 02	04 01	26 01	40 02	40 04	40 07	40 08	43 05	48 01
ζ	3	1.03	2.6	1.01	4	3	4.5	1.1	1.35	1.01
λ	1.01	1.21	1.01	1.05	1.1	1.05	1.01	1.05	1.3	1.05
κ	2.9	2.6	2	1.7	1.6	1.8	2.5	3.5	2.2	2.95
α	1	0.9	1.6	1	1.6	0.5	1.1	1.1	1.01	0.8

Note that ζ is rather sensitive to the selection of the starting time of the oscillation and we assume that the cooling time is equal to oscillation time. Whilst conducting the fits, virtually any values of $\zeta \pm 0.2$, $\lambda \pm 0.05$, $\kappa \pm 0.2 \pm \varepsilon_\kappa$, $\alpha \pm 0.1 \pm \varepsilon_\alpha$, where ε with subscript denotes the errors associated with variation of ζ provided sufficiently good approximations to the observed values, however, the above particular values were chosen to follow the measured damping trend better. Given that there might be an error in the estimation of the starting time of damping, one should pay extra care of determining ζ in the vicinity of ζ = 1, due to the ratio of internal and external densities being susceptible to changes in this interval. The combination of λ, κ, and α are key for the speed of decay of the amplitude. In this study, these values were treated as parameters and further measurements should be made to accurately determine κ and α in the future. We note that Event 40 02 was studied previously by Nelson et al. (2019), however, here we analyzed a longer time-period, therefore, explaining the difference in ζ.

Table 3 provides the comparison with previous models, we could see that inclusion of cooling to Events 03 02, 26 01, 40 02, 40 07 with oscillation time been equal to the oscillation time could lead the cooling theoretical model to have better approximations

to the damping profiles than exponential and Gaussian fits, in case only extremum points (i.e. amplitude maxima) are taken as the point of reference. If instead we analyze the overall damping profile (i.e. calculate the χ^2 values at all time-steps), then Events 03 01, 03 02, 04 01, 26 01, 40 02, 40 07, 43 05 are approximated better by the cooling model, rather than exponential or Gaussian fits. We should note that the goodness of fit could be further improved in the cooling model if we were to put more stress on deviation from the observed data instead of focusing on finding the turning points. However, we should mention that position of turning point is crucial for estimation for values of ζ. Furthermore, changing the ration between oscillation time and cooling time could improve significantly the goodness of fit as was described in Event 03 01.

4 CONCLUSION

In this article, we have further demonstrated the promise of the theory developed by Shukhobodskiy et al. (2018) by applying it to 10 driven kink-mode oscillations. These events were sampled by the SDO/AIA instrument and were randomly selected from the population identified to have complex damping profiles in the statistical study of Goddard et al. (2016). Space-time diagrams were constructed for each oscillation before the edges of the loops through time were determined by employing the Canny edged-detection method (see **Figure 1**). The mid-point between the edges was defined as the central axis of the oscillating loop for each time-step. The background trends were then subtracted from each oscillation using spline fitting before the detrended data were then fitted with a series of Gaussian functions. The results of the application of these steps to the oscillations can be seen in **Figure 2**.

Next, we plotted the absolute values of the amplitude variation of the kink-mode oscillations through time in **Figure 3**. Some oscillations displayed clear deviations from the usual Gaussian or exponential damping profiles even at this stage. Specifically, five (Events 04 01, 40 02, 40 04 (LC), 40 07, and 43 05) of the 10 oscillations studied here displayed evidence of increases in amplitude through time. Such amplification was shown to be possible during oscillations of cooling loops by Ruderman (2011b), Shukhobodskiy and Ruderman (2018) and has been reported before in observations by Nelson et al. (2019). Using an iterative approach, we then constructed best fits for the parameters defined in **Eq. 5** such that the difference between the observed and theoretical damping profiles was minimized. In **Figure 4** it was shown that this theoretical model provides qualitatively reasonable approximations for the damping of kink oscillations of coronal loops for nine of the 10 cases (all except Event 40 04 [LC]). This result indicates that cooling should be studied in more detail in future research. Additionally, we have also shown that the model is capable of capturing the properties of fitting both simple Gaussian and exponential profiles, depending on the ratio of external and internal densities, ζ, at the loop foot-points. Furthermore, for sufficiently large loops with $\kappa \geq 1.6$, the shape of the damping profile is determined by this ratio. In the case where cooling is present, for the small values of ζ the profile would be Gaussian, while for large values of ζ it would be exponential. All values in-between would be a combination of both.

It was shown by Shukhobodskiy et al. (2018) that higher expansion factors of coronal loops could result in overall amplification of the first part of the oscillation eventually resulting in Gaussian decay of the amplitude profile. Thus studying complex damping profiles could allow us to extract interesting seismological information, such as the ratios of densities at foot-points. Furthermore, the information presented in **Figure 6** suggests, that lower ratios of internal and external densities have higher amplitude and period. One of the reasons why this could happen is that the coronal loops investigated are lighter and less disturbance created by the flare is needed to disturb the system more prominently. A larger statistical study and more targeted observations with spectral instruments suitable for providing density diagnostics (such as IRIS) should be used to study this potenatial result in more detail in the future.

Overall, we presented an alternative approach to model more complex damping profiles that deviate from the widely studied Gaussian and exponential decays. A number of examples of such deviation were addressed in this study, thus strengthening the claim made by Nelson et al. (2019) that the effect of cooling should be further considered for analyzing oscillations of coronal loops. This is in agreement with some earlier studies, e.g. by Morton and Erdélyi (2009), Morton and Erdélyi (2010). Furthermore, in the case of strong damping the theoretical model proposed by Shukhobodskiy et al. (2018) is able to provide seismological information, just from the damping profile alone. For some events, the cooling model demonstrated significant improvement over standard Gaussian on exponential fitting when χ^2 goodness of fits were calculated. We should note that results employed from Shukhobodskiy et al. (2018) model was only studied on the fundamental mode only. However, additional studies with inclusion of mode mixing would allow comparison with other fitting techniques that allowed multiple harmonics to be present, which could further unveil details regarding kink oscillations of coronal loops. Unfortunately, for less dominant damping more parameters need to be determined from observation in order to extract the information about the kink oscillations of coronal loops.

Although little evidence is presented about the actual cooling for the events studied here, it is possible that the gradual fading of the intensity of several coronal loops presented in **Figure 1** (specifically for Events 03 01, 04 01, and 43 05) may imply that some thermal evolution (either heating or cooling) is present. In a future work, it would be worthwhile to analyze oscillations within loops which are undergoing specific processes linked to cooling, such as coronal rain (Antolin et al., 2015) or the associated high velocity transition region downflows (see, for example, Nelson et al., 2020b, Nelson et al., 2020a and literature within), to understand whether abnormal amplitude profiles through time (such as those studied here) are present. Additionally, it would be worthwhile to develop further the

analytical methods, which then could help to extract additional information about the kink oscillation of coronal loops, in order to optimize this theory for the application of solar magneto-seismology to kink-mode oscillations.

DATA AVAILABILITY STATEMENT

Publicly available datasets were analyzed in this study. This data can be found here: https://jsoc.stanford.edu.

AUTHOR CONTRIBUTIONS

AS and CN conceived the study. DS and AS conducted the data analysis, with DS having a major contribution to the analysis. All authors consulted on the interpretation of results. DS, AS, and CN drafted the manuscript. All authors read, discussed and commented on the draft. RE lead the research overall.

FUNDING

DS is grateful to the University of Sheffield for the support received. AS is thankful to Interreg Northwest Europe for the support received to conduct this research through grant number: NWE847. CN is thankful to the Science and Technology Facilities Council (STFC) for the support received to conduct this research through grant number: ST/P000304/1. RE is grateful to STFC (UK, grant number ST/M000826/1). RE also acknowledges support from the Chinese Academy of Sciences President's International Fellowship Initiative (PIFI, grant number 2019VMA0052) and The Royal Society (grant nr IE161153).

ACKNOWLEDGMENTS

SDO/AIA data are courtesy of NASA/SDO and the AIA science team. We thank S. Krishna Prasad for making their slit creation code available to us.

REFERENCES

Al-Ghafri, K. S., and Erdélyi, R. (2013). Effect of variable background on an oscillating hot coronal loop. *Sol. Phys.* 283, 413–428. doi:10.1007/s11207-013-0225-8

Al-Ghafri, K. S., Ruderman, M. S., Williamson, A., and Erdélyi, R. (2014). Longitudinal Magnetohydrodynamics oscillations in dissipative, cooling coronal loops. *Astrophys. J.* 786, 36. doi:10.1088/0004-637X/786/1/36

Andries, J., van Doorsselaere, T., Roberts, B., Verth, G., Verwichte, E., and Erdélyi, R. (2009). Coronal seismology by means of kink oscillation overtones. *Space Sci. Rev.* 149, 3–29. doi:10.1007/s11214-009-9561-2

Anfinogentov, S., Nisticò, G., and Nakariakov, V. M. (2013). Decay-less kink oscillations in coronal loops. *Astron. Astrophys.* 560, A107. doi:10.1051/0004-6361/201322094

Antolin, P., Vissers, G., Pereira, T. M. D., Rouppe van der Voort, L., and Scullion, E. (2015). The multithermal and multi-stranded nature of coronal rain. *Astrophys. J.* 806, 81. doi:10.1088/0004-637X/806/1/81

Aschwanden, M. J., Fletcher, L., Schrijver, C. J., and Alexander, D. (1999). Coronal loop oscillations observed with the transition region and coronal explorer. *Astrophys. J.* 520, 880–894. doi:10.1086/307502

Aschwanden, M. J., and Schrijver, C. J. (2011). Coronal loop oscillations observed with atmospheric imaging assembly—kink mode with cross-sectional and density oscillations. *Astrophys. J.* 736, 102. doi:10.1088/0004-637X/736/2/102

Aschwanden, M. J., and Terradas, J. (2008). The effect of radiative cooling on coronal loop oscillations. *Astrophys. J. Lett.* 686, L127. doi:10.1086/592963

De Pontieu, B., Title, A. M., Lemen, J. R., Kushner, G. D., Akin, D. J., Allard, B., et al. (2014). The Interface region imaging Spectrograph (IRIS). *Sol. Phys.* 289, 2733–2779. doi:10.1007/s11207-014-0485-y

Dymova, M. V., and Ruderman, M. S. (2006). Resonantly damped oscillations of longitudinally stratified coronal loops. *Astron. Astrophys.* 457, 1059–1070. doi:10.1051/0004-6361:20065051

Edwin, P. M., and Roberts, B. (1983). Wave propagation in a magnetic cylinder. *Sol. Phys.* 88, 179–191. doi:10.1007/BF00196186

Erdélyi, R., Al-Ghafri, K. S., and Morton, R. J. (2011). Damping of longitudinal magneto-acoustic oscillations in slowly varying coronal plasma. *Sol. Phys.* 272, 73–89. doi:10.1007/s11207-011-9795-5

Erdelyi, R., and Goossens, M. (1995). Resonant absorption of Alfven waves in coronal loops in visco-resistive MHD. *Astron. Astrophys.* 294, 575–586. doi:10.1063/1.1343090

Erdelyi, R., and Goossens, M. (1994). Viscous computations of resonant absorption of MHD waves in flux tubes by fem. *Astrophys. Space Sci.* 213, 273–298. doi:10.1007/BF00658215

Goddard, C. R., and Nakariakov, V. M. (2016). Dependence of kink oscillation damping on the amplitude. *Astron. Astrophys.* 590, L5. doi:10.1051/0004-6361/201628718

Goddard, C. R., Nisticò, G., Nakariakov, V. M., and Zimovets, I. V. (2016). A statistical study of decaying kink oscillations detected using SDO/AIA. *Astron. Astrophys.* 585, A137. doi:10.1051/0004-6361/201527341

Goddard, C. R., and Nisticò, G. (2020). Temporal evolution of oscillating coronal loops. *Astron. Astrophys.* 638, A89. doi:10.1051/0004-6361/202037467

Goddard, C. R., Pascoe, D. J., Anfinogentov, S., and Nakariakov, V. M. (2017). A statistical study of the inferred transverse density profile of coronal loop threads observed with SDO/AIA. *Astron. Astrophys.* 605, A65. doi:10.1051/0004-6361/201731023

Goossens, M., Andries, J., and Aschwanden, M. J. (2002). Coronal loop oscillations. An interpretation in terms of resonant absorption of quasi-mode kink oscillations. *Astron. Astrophys.* 394, L39. doi:10.1051/0004-6361:20021378

Goossens, M., Erdélyi, R., and Ruderman, M. S. (2011). Resonant MHD waves in the solar atmosphere. *Space Sci. Rev.* 158, 289–338. doi:10.1007/s11214-010-9702-7

Goossens, M., Hollweg, J. V., and Sakurai, T. (1992). Resonant behavior of MHD waves on magnetic-flux tubes. 3. Effect of equilibrium-flow. *Sol. Phys.* 138, 233–255. doi:10.1007/BF00151914

Hollweg, J. V., and Yang, G. (1988). Resonant-absorption of compressible magnetohydrodynamic waves at thin surfaces. *Comput. Phys. Rep.* 93, 5423–5436. doi:10.1029/JA093iA06p05423

Hood, A. W., Ruderman, M., Pascoe, D. J., De Moortel, I., Terradas, J., and Wright, A. N. (2013). Damping of kink waves by mode coupling. I. Analytical treatment. *Astron. Astrophys.* 551, A39. doi:10.1051/0004-6361/201220617

Ishikawa, R. T., Katsukawa, Y., Antolin, P., and Toriumi, S. (2020). Temporal and spatial scales in coronal rain revealed by UV imaging and spectroscopic observations. *Sol. Phys.* 295, 53. doi:10.1007/s11207-020-01617-z

Kleint, L., Antolin, P., Tian, H., Judge, P., Testa, P., De Pontieu, B., et al. (2014). Detection of supersonic downflows and associated heating events in the transition region above sunspots. *Astrophys. J. Lett.* 789, L42. doi:10.1088/2041-8205/789/2/L42

Klimchuk, J. A. (2000). Cross-Sectional properties of coronal loops. *Sol. Phys.* 193, 53–75. doi:10.1023/A:1005210127703

Krishna Prasad, S., Banerjee, D., and Singh, J. (2012). Oscillations in active region fan loops: observations from EIS/hinode and AIA/SDO. *Sol. Phys.* 281, 67–85. doi:10.1007/s11207-012-0098-2

Krishna Prasad, S., Jess, D. B., Klimchuk, J. A., and Banerjee, D. (2017). Unravelling the components of a multi-thermal coronal loop using magnetohydrodynamic seismology. *Astrophys. J.* 834, 103. doi:10.3847/1538-4357/834/2/103

Kumar, P., Cho, K. S., Chen, P. F., Bong, S. C., and Park, S. H. (2013). Multiwavelength study of a solar eruption from AR NOAA 11112: II. Large-scale coronal wave and loop oscillation. *Sol. Phys*. 282, 523–541. doi:10.1007/s11207-012-0158-7

Kuridze, D., Morton, R. J., Erdélyi, R., Dorrian, G. D., Mathioudakis, M., Jess, D. B., et al. (2012). Transverse oscillations in chromospheric mottles. *Astrophys. J.* 750, 51. doi:10.1088/0004-637X/750/1/51

Lemen, J. R., Title, A. M., Akin, D. J., Boerner, P. F., Chou, C., Drake, J. F., et al. (2012). The atmospheric imaging assembly (AIA) on the solar dynamics observatory (SDO). *Sol. Phys*. 275, 17–40. doi:10.1007/s11207-011-9776-8

López Fuentes, M. C., Klimchuk, J. A., and Mandrini, C. H. (2007). The temporal evolution of coronal loops observed by GOES SXI. *Astrophys. J.* 657, 1127–1136. doi:10.1086/510662

Morton, R. J., and Erdélyi, R. (2010). Application of the theory of damping of kink oscillations by radiative cooling of coronal loop plasma. *Astron. Astrophys*. 519, A43. doi:10.1051/0004-6361/201014504

Morton, R. J., and Erdélyi, R. (2009). Transverse oscillations of a cooling coronal loop. *Astrophys. J.* 707, 750–760. doi:10.1088/0004-637X/707/1/750

Morton, R. J., Hood, A. W., and Erdélyi, R. (2010). Propagating magneto-hydrodynamic waves in a cooling homogenous coronal plasma. *Astron. Astrophys*. 512, A23. doi:10.1051/0004-6361/200913365

Morton, R. J., Verth, G., Jess, D. B., Kuridze, D., Ruderman, M. S., Mathioudakis, M., et al. (2012). Observations of ubiquitous compressive waves in the Sun's chromosphere. *Nat. Commun*. 3, 1315. doi:10.1038/ncomms2324

Nakariakov, V. M., Ofman, L., Deluca, E. E., Roberts, B., and Davila, J. M. (1999). TRACE observation of damped coronal loop oscillations: implications for coronal heating. *Science*. 285, 862–864. doi:10.1126/science.285.5429.862

Nelson, C. J., Krishna Prasad, S., and Mathioudakis, M. (2020a). Evolution of downflows in the transition region above a sunspot over short time-scales. *Astron. Astrophys*. 640, 13. doi:10.1051/0004-6361/202038155

Nelson, C. J., Krishna Prasad, S., and Mathioudakis, M. (2020b). Evolution of supersonic downflows in a sunspot. *Astron. Astrophys*. 636, A35. doi:10.1051/0004-6361/201937357

Nelson, C. J., Shukhobodskiy, A. A., Erdélyi, R., and Mathioudakis, M. (2019). The effect of cooling on driven kink oscillations of coronal loops. *Frontiers in Astronomy and Space Sciences*. 6, 45. doi:10.3389/fspas.2019.00045

Pascoe, D. J., Goddard, C. R., and Nakariakov, V. M. (2016a). Spatially resolved observation of the fundamental and second harmonic standing kink modes using SDO/AIA. *Astron. Astrophys*. 593, A53. doi:10.1051/0004-6361/201628784

Pascoe, D. J., Goddard, C. R., Nisticò, G., Anfinogentov, S., and Nakariakov, V. M. (2016b). Damping profile of standing kink oscillations observed by SDO/AIA. *Astron. Astrophys*. 585, L6. doi:10.1051/0004-6361/201527835

Pascoe, D. J., Hood, A. W., and Van Doorsselaere, T. (2019). Coronal loop seismology using standing kink oscillations with a lookup table. *Frontiers in Astronomy and Space Sciences*. 6, 22. doi:10.3389/fspas.2019.00022

Pascoe, D. J., Russell, A. J. B., Anfinogentov, S. A., Simões, P. J. A., Goddard, C. R., Nakariakov, V. M., et al. (2017). Seismology of contracting and expanding coronal loops using damping of kink oscillations by mode coupling. *Astron. Astrophys*. 607, A8. doi:10.1051/0004-6361/201730915

Pascoe, D. J., Smyrli, A., and Van Doorsselaere, T. (2020). Tracking and seismological analysis of multiple coronal loops in an active region. *Astrophys. J.* 898, 126. doi:10.3847/1538-4357/aba0a6

Ruderman, M. S., and Erdélyi, R. (2009). Transverse oscillations of coronal loops. *Space Sci. Rev*. 149, 199–228. doi:10.1007/s11214-009-9535-4

Ruderman, M. S. (2011b). Resonant damping of kink oscillations of cooling coronal magnetic loops. *Astron. Astrophys*. 534, A78. doi:10.1051/0004-6361/201117416

Ruderman, M. S., and Roberts, B. (2002). The damping of coronal loop oscillations. *Astrophys. J.* 577, 475–486. doi:10.1086/342130

Ruderman, M. S., Shukhobodskaya, D., and Shukhobodskiy, A. A. (2019). Resonant damping of propagating kink waves in non-stationary, longitudinally stratified, and expanding solar waveguides. *Front. Astron. Space Sci*. 6, 10. doi:10.3389/fspas.2019.00010

Ruderman, M. S., Shukhobodskiy, A. A., and Erdélyi, R. (2017). Kink oscillations of cooling coronal loops with variable cross-section. *Astron. Astrophys*. 602, A50. doi:10.1051/0004-6361/201630162

Ruderman, M. S., and Terradas, J. (2013). Damping of coronal loop kink oscillations due to mode conversion. *Astron. Astrophys*. 555, A27. doi:10.1051/0004-6361/201220195

Ruderman, M. S. (2011a). Transverse oscillations of coronal loops with slowly changing density. *Sol. Phys*. 271, 41–54. doi:10.1007/s11207-011-9772-z

Ruderman, M. S., Verth, G., and Erdélyi, R. (2008). Transverse oscillations of longitudinally stratified coronal loops with variable cross section. *Astrophys. J.* 686, 694–700. doi:10.1086/591444

Ryutov, D. A., and Ryutova, M. P. (1976). Sound oscillations in a plasma with "magnetic filaments". *J. Exp. Theor. Phys*. 43, 491.

Samanta, T., Tian, H., and Prasad Choudhary, D. (2018). Statistical investigation of supersonic downflows in the transition region above sunspots. *Astrophys. J.* 859, 158. doi:10.3847/1538-4357/aabf37

Shukhobodskiy, A. A., Ruderman, M. S., and Erdélyi, R. (2018). Resonant damping of kink oscillations of thin cooling and expanding coronal magnetic loops. *Astron. Astrophys*. 619, A173. doi:10.1051/0004-6361/201833714

Shukhobodskiy, A. A., and Ruderman, M. S. (2018). Resonant damping of kink oscillations of thin expanding magnetic tubes. *Astron. Astrophys*. 615, A156. doi:10.1051/0004-6361/201732396

Straus, T., Fleck, B., and Andretta, V. (2015). A steady-state supersonic downflow in the transition region above a sunspot umbra. *Astron. Astrophys*. 582, A116. doi:10.1051/0004-6361/201525805

Wang, T., Ofman, L., Davila, J. M., and Su, Y. (2012). Growing transverse oscillations of a multistranded loop observed by SDO/AIA. *Astrophys. J. Lett*. 751, L27. doi:10.1088/2041-8205/751/2/L27

Watko, J. A., and Klimchuk, J. A. (2000). Width variations along coronal loops observed by TRACE. *Sol. Phys*. 193, 77–92. doi:10.1023/A:1005209528612

Winebarger, A. R., and Warren, H. P. (2005). Cooling active region loops observed with SXT and TRACE. *Astrophys. J.* 626, 543–550. doi:10.1086/429817

Zimovets, I. V., and Nakariakov, V. M. (2015). Excitation of kink oscillations of coronal loops: statistical study. *Astron. Astrophys*. 577, A4. doi:10.1051/0004-6361/201424960

Conflict of Interest: The authors declare that the research was conducted in the absence of any commercial or financial relationships that could be construed as a potential conflict of interest.